First Mandatory Assignment

MEK4420

Simon Lederhilger

January 28th 2025

Scope of the assignment

The assignment at hand is to solve the integral equation

$$\pi\phi(\boldsymbol{\mathcal{HC}}) = \int_{\partial\Omega} \left(\phi\partial_{\hat{\boldsymbol{n}}}\,\mathrm{G} - \mathrm{G}\,\partial_{\hat{\boldsymbol{n}}}\phi\right)\mathrm{d}S$$

by numerical implementation, calculate the added mass, and compare the results to theoretical values. The shapes to be considered are a circle, ellipses of aspect ratios $a/b = 1/2$ and $a/b = 1/10$, and a square. As we shall need to consider the theoretical values of these shapes' added masses, these will be derived. Although the lecture notes found in the repository in which this assignment is located already have an explanation of added mass, albeit rather heuristically inclined, a different approach will be taken for this assignment. This assignment will furthermore function as documentation for the `Python`-code developed for the purpose of calculating added mass.

Added mass on bodies

To gain insight into what *added mass* actually represents, the reader is highly encouraged to read the 1953 paper of Charles G. Darwin *Note on Hydrodynamics.*[1] It is therein demonstrated that bodies moving in an ideal fluid cause drift of the fluid, and that the drift volume is equivalent to the added mass. Authors in older works usually provide the kinetic energy of the system instead of the added mass, as the added mass may be inferred. Consider a body in an unbounded fluid being accelerated such that its energy is T_{body}. We know this induces a drift in the fluid, whose energy we shall label T_{fluid}, and that the total energy then is $T = T_{\text{body}} + T_{\text{fluid}}$. Consider now a fluid flow with potential Φ. Letting ϱ denote the fluid density, the kinetic energy of the fluid is then

$$T_{\text{fluid}} = \frac{\varrho}{2}\int_{\Omega} q^2\,\mathrm{d}V, \quad q = |\nabla\Phi| = \frac{\mathrm{d}w}{\mathrm{d}\mathcal{Z}}\frac{\mathrm{d}w^*}{\mathrm{d}\mathcal{Z}^*}, \quad (1)$$

integrating over the entire fluid domain Ω, excluding the body. The complex formulation will be necessary later, but we pay no attention to it for the time being. The speed q may be related to the velocity magnitude U by assuming the modal superposition $\Phi(t;\boldsymbol{x}) = \boldsymbol{U}(t)\cdot\boldsymbol{\phi}(\boldsymbol{x})$. Drawing upon the physical interpretation of kinetic energy, it is apparent that in general, it may be expressed as

$$T = \frac{(m+m')U^2}{2}, \qquad m' = \varrho k A,$$

where we note the added mass m' depends on the area of the body A, and an inertia coefficient k. This coefficient indicates the orientation of the body in relation to the direction of motion—we can imagine an ellipse moving parallel to its major axis will cause less drift in the fluid than it would moving perpendicular to it. That will at least that will be shown to be the case, mathematically. One may confirm the dependency on orientation readily in one's own kitchen—if imagination does not satisfy—by filling a container with water, and holding a spoon so that the bowl is submerged, moving it every which way. One shall find that moving the spoon with the bowl perpendicular to the direction of motion requires more work than moving it with the bowl parallel to the direction of motion. In fact, maintaining such work with a force F, we have that $FU = \partial_t T_{\text{fluid}}$, and extending Blasius' theorem,[2] we have that

$$\boldsymbol{F} = -\partial_t\boldsymbol{U}\colon \varrho\int_{\partial\Omega}\boldsymbol{\phi}\otimes\hat{\boldsymbol{n}}\,\mathrm{d}S,$$

where S is the contour of the body, and $\otimes$ denotes the outer product. $\boldsymbol{\phi}$ is a vector containing the modes of translation,

$$\boldsymbol{\phi}(\boldsymbol{x},t) = \phi_1\hat{\boldsymbol{\imath}} + \phi_2\hat{\boldsymbol{\jmath}} + \phi_6\hat{\boldsymbol{\omega}}_{\hat{\boldsymbol{k}}}.$$

It will be shown later that this formulation is indeed equivalent to the complex variable formulation of equation (1), and not just some heuristic deduction from the oughts of Newtonian physics.

[1] [3] Darwin (1953)

[2] [7] Milne–Thomson, pp.255–256

This is the very same formulation found in the lecture notes, yielding—what heusristically ought to be named—the *added mass* tensor in terms of the following integral, which will be used for the numerical calculation.

$$\mathfrak{m} = \varrho \int_{\partial\Omega} \boldsymbol{\phi} \otimes \hat{\boldsymbol{n}} \, \mathrm{d}S \tag{2}$$

Discrete integral equation

The integral equation

Since the fluid is ideal, we may reduce the incompressibility condition to the Laplace equation,

$$\nabla^2 \phi = 0, \qquad \text{in } \Omega.$$

It may be shown with the product rule that for any harmonic functions $\phi, \psi \in \Omega$,

$$\nabla \cdot \big(\phi \nabla\psi - \psi\nabla\phi\big) \equiv 0,$$

which upon being integrated over Ω and applying Gauss' divergence theorem, yields

$$\int_{\partial\Omega} \big(\phi\nabla\psi - \psi\nabla\phi\big) \cdot \hat{\boldsymbol{n}} \, \mathrm{d}S = 0.$$

Since we only need the values of the potential on the contour $\partial\Omega$ to calculate the added mass, we look to Green functions, which are defined through the property that they satisfy some differential operator except at some point $\boldsymbol{\varkappa} \in \mathrm{Q}$, where $\mathrm{Q} = \Omega \cup \partial\Omega$, such that

$$\nabla^2 \mathrm{G} = \delta(\boldsymbol{x} - \boldsymbol{\varkappa}), \qquad \boldsymbol{x} \in \mathrm{Q}.$$

In other words, the Green function is almost harmonic, and we expect the above integral should hold except at the pole. The Green function for the Laplace operator is the natural logarithm,

$$\mathrm{G}(\boldsymbol{x}) = \ln r, \qquad r = |\boldsymbol{x} - \boldsymbol{\varkappa}|,$$

which has a pole at $\boldsymbol{\varkappa}$. Now, by placing $\boldsymbol{\varkappa} \in \partial\Omega$, we find by the Cauchy principal value,[1] that

$$-\pi\phi(\boldsymbol{\varkappa}) + \mathrm{pv}\int_{\partial\Omega} \phi\partial_{\hat{\boldsymbol{n}}} \ln r \, \mathrm{d}S = \mathrm{pv}\int_{\partial\Omega} \partial_{\hat{\boldsymbol{n}}}\phi \ln r \, \mathrm{d}S.$$

An outline of calculating the principal value is found in the lecture notes from January 21st. We drop the principal value notation for brevity.

The boundary element method

To implement the integral equation numerically, we utilize the boundary element method. In essence, we distribute a number of nodes along the boundary on which we would like to solve the integral equation, and linearily interpolate the points to approximate boundary. If the number of nodes is N, then we have $\partial\Omega \sim S = \{S_n \colon n \leq N,\, n \in \mathbb{Z}^+\}$. We then assume the potential is constant on each of S_n, equal to the potential evaluated at the midpoint, labelling this ${\phi_j}^n \equiv \phi_j(\boldsymbol{\varkappa}_n)$. Now, since the normal derivative of the potential also must be zero on the line segments, the integrals in the integral equation may be approximated by the sum of the integrals evaluated over wach of the line segments as follows.

$$\int_{\partial\Omega} \phi\partial_{\hat{\boldsymbol{n}}} \ln r \, \mathrm{d}S \approx \sum_{n=1}^{N} \phi^n \int_{S_n} \partial_{\hat{\boldsymbol{n}}} \ln r \, \mathrm{d}S \tag{3}$$

$$\int_{\partial\Omega} \ln r \partial_{\hat{\boldsymbol{n}}}\phi \, \mathrm{d}S \approx \sum_{n=1}^{N} \hat{\boldsymbol{n}}^n \int_{S_n} \ln r \, \mathrm{d}S \tag{4}$$

It should be quite clear that the integral equation may then be written as the matrix equation

$$-\pi\phi^n + \sum_{n=1}^{N} \phi^n \mathtt{\Theta}_{m,n} = \sum_{n=1}^{N} \hat{\boldsymbol{n}}^n \mathtt{h}_{m,n},$$

where we have set $\mathtt{\Theta}_{m,n}$ and $\mathtt{h}_{m,n}$ to be approximations of equations (3) and (4), respectively.

The logarithmic gradient

It turns out the integral of the gradient of the logarithm can be determined using complex analysis. The gradient is an operator from the real numbers into the vector space of the complex numbers, in the sense that

$$\nabla u(\mathfrak{z}) = \partial_x u(\mathfrak{z}) + i\partial_z u(\mathfrak{z}), \qquad \mathfrak{z} = x + iz.$$

Considering now an analytic function $\boldsymbol{u} = u + iv$, its complex derivative is given by $\partial_{\mathfrak{z}}\boldsymbol{u} = \partial_x u + i\partial_x v$, which by the Cauchy–Riemann equations yields that $\partial_{\mathfrak{z}}\boldsymbol{u} = \nabla u^*$. We recall that the principal value of the complex logarithm is given by $\log(\mathfrak{z}) = \ln|\mathfrak{z}| + i\,\mathrm{Arg}(\mathfrak{z})$,[2] so that $\partial_{\mathfrak{z}} \log(\mathfrak{z}) = \nabla \ln|\mathfrak{z}|^*$.

Now, for a curve parametrized by $\lambda(s)$, the normal vector $\hat{\boldsymbol{n}}$ may be represented by[3]

$$\nu(s) = -i\lambda'(s) = \frac{\mathrm{d}z}{\mathrm{d}s} - i\frac{\mathrm{d}x}{\mathrm{d}s} = -i\frac{\mathrm{d}\mathfrak{z}}{\mathrm{d}s}. \tag{5}$$

The inner product may be defined such that $\boldsymbol{u}\cdot\hat{\boldsymbol{n}} = \mathrm{Re}\,(\boldsymbol{u}^*\nu(s))$. We then have that

$$\partial_{\hat{\boldsymbol{n}}} \ln r = \mathrm{Re}\left(-i\frac{\mathrm{d}\mathfrak{z}}{\mathrm{d}s}\partial_{\mathfrak{z}} \log(\mathfrak{z} - \boldsymbol{\varkappa}_m)\right).$$

[1] [5] Lavrentev & Šabat, pp.331–332
[2] [5] Lavrentev & Šabat, p.30
[3] [6] Markuševič, p.175

Since the line segment is parameterized by s, the differential element may then be taken over $\mathcal{z}$. By the linearity of the $\mathrm{Re}\,(\star)$ operator, we have that

$$\int_{S_n} \partial_{\hat{\boldsymbol{n}}} \ln r \,\mathrm{d}S = -\,\mathrm{Re}\, i \int_{\boldsymbol{x}_{n-1}}^{\boldsymbol{x}_n} \frac{\mathrm{d}}{\mathrm{d}\mathcal{z}} \log\left(\mathcal{z} - \mathcal{zc}_m\right) \mathrm{d}\mathcal{z}.$$
$$= \mathrm{Arg}\left(\frac{\boldsymbol{x}_{n-1} - \mathcal{zc}_m}{\boldsymbol{x}_n - \mathcal{zc}_m}\right).$$

This is just the angle between $\boldsymbol{x}_n$, $\mathcal{zc}_m$, and $\boldsymbol{x}_{n-1}$.

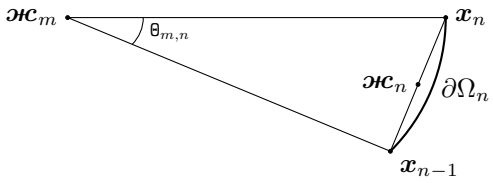

Figure 1: Visualization of $\Theta_{m,n}$. Here $\partial\Omega_n$ denotes the segment along $\partial\Omega$ between $\boldsymbol{x}_n$ and $\boldsymbol{x}_{n-1}$.

If $\boldsymbol{x}$ then is the array of the N nodes x_n, we can fill the matrix Θ with the arguments with `for`-loops, which is implemented in the `assemble` method in the `IntegralEquation` class, found in `integralequation.py`. The class variable $\boldsymbol{\mathcal{x}} = {}^1\!/_2(\boldsymbol{x}_n + \boldsymbol{x}_{n-1})$, containing the aforementioned midpoints is created upon initialization of the class, since multiple methods make use of it.

Algorithm 1 Assemble Θ

```
for m, n ≤ N do
    if m = n then
        Θ_mn ← −π
    else
        Θ_mn ← angle( (x[n−1] − x_c[m]) / (x[n] − x_c[m]) )
    end if
end for
```

This method essentially assembles the entire left-hand side of the integral equation, so that we may simply solve $\phi = \Theta^{-1}\mathtt{h}$.

Gauss–Legendre quadrature

To construct $\mathtt{h}$, we evaluate the integral of the logarithm using quadrature. For an integral on the real line, Gaussian quadrature approximates it by transforming it to the unit ball,

$$\int_a^b y(x)\,\mathrm{d}x \mapsto \int_{-1}^{1} \eta(\xi)\,\mathrm{d}\xi,$$

where $\eta(\xi) \equiv y\big(x(\xi)\big)\partial_\xi x$, a change of variables such that $x(-1) = a$ and $x(1) = b$. Gauss–Legendre quadrature of order K has us approximating this integral by

$$\sum_{k=1}^{K} w_k \eta(\xi_k), \quad w_k = \frac{2}{\left(1-{\xi_k}^2\right)\left(\mathrm{P}'_K(\xi_k)\right)^2},$$

where P_K is the K^{th} Legendre polynomial, ξ_k is its k^{th} zero, and w_k is the corresponding weight. The Legendre polynomials are given by the recursion formula[1]

$$(n+1)\,\mathrm{P}_{n+1}(\xi) = (2n+1)\xi\,\mathrm{P}_n(\xi) - n\,\mathrm{P}_{n-1}(\xi),$$

where we have defined $\mathrm{P}_0(\xi) = 1$, $\mathrm{P}_1(\xi) = \xi$. From the recurrence relation we find the 2^{nd} order Legendre polynomial, its zeros, and its weights:

$$\mathrm{P}_2(\xi) = \frac{3x^2-1}{2}, \quad \xi_k = (-1)^k\frac{\sqrt{3}}{3}, \quad w_k = 1$$

We find below that we have no use for the 3^{rd} polynomial, but we may use the 4^{th}, for which we have

$$\mathrm{P}_4(\xi) = \frac{105\xi^4 - 90\xi^2 + 9}{24}, \quad \xi_k = \pm\sqrt{\frac{3 \pm 2\sqrt{{}^6\!/_5}}{7}}.$$

The zeros ξ_k are readily found by solving the biquadratic equation, the the signs may be chosen independently, yielding four roots. As for the wieghts, they are found after some algebraic manipulation, and turn out to be

$$w_k = \frac{18 \pm \sqrt{30}}{36}.$$

Instead of ginning up some elaborate mathematical expression to relate the roots to their respective weights, an illustration is provided in figure 2 below.

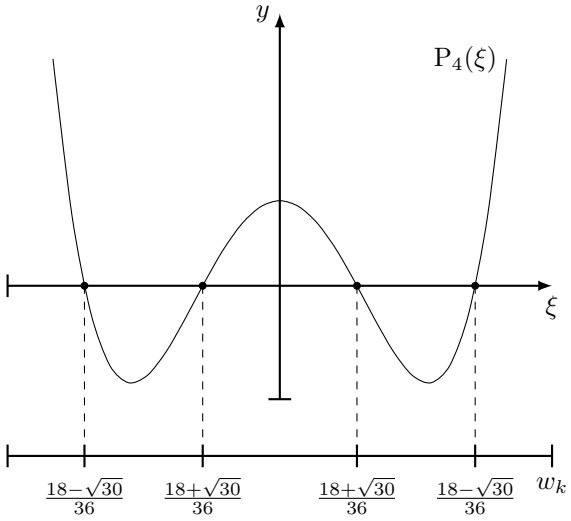

Figure 2: The fourth Legendre polynomial plotted, with the weights associated with its four roots indicated.

To calculate the target integral by quadrature, we may parametrize the variable of integration by writing that the line segment S_n is given by

$$\mathcal{z}(\xi) = \left(\frac{\boldsymbol{x}_n - \boldsymbol{x}_{n-1}}{2}\right)\xi + \left(\frac{\boldsymbol{x}_n + \boldsymbol{x}_{n-1}}{2}\right),$$

[1] [1] Abramowitz & Stegun, 22.7.10, p.782

where $\xi \in [-1, 1]$. We recognize the rightmost term above as $\boldsymbol{\varkappa}_n$, and for brevity, we write that $\boldsymbol{x}_n - \boldsymbol{x}_{n-1} = \delta\boldsymbol{x}$, which is implemented as the method `IntegralEquation.Δx`. Now $\ln|\mathcal{Z}(\xi)|$ clearly is a function from the real numbers into the real numbers, so we may use the fact that for any real valued function over the complex plane,

$$\int_C f(\mathcal{Z})\,\mathrm{d}S = \int_a^b f\big(\mathcal{Z}(\xi)\big)|\mathcal{Z}'(\xi)|\,\mathrm{d}\xi.$$

We calculate that $|\mathcal{Z}'(\xi)| = {}^1\!/_2|\delta\boldsymbol{x}|$, which is implemented as the class variable `dS` in the `Quadrature` class of `quadrature.py`. It should now be clear that we may not use an odd order quadrature scheme, as the diagonal of `h` will entail evaluating the logarithm at zero, since $\xi_k = 0$ will always be a root of an odd order LEGENDRE polynomial.

We again utilize the fact that $\operatorname{Re}\big(\log\mathcal{Z}\big) = \ln|\mathcal{Z}|$, so that

$$\int_{S_n} \ln r\,\mathrm{d}S = \frac{|\delta\boldsymbol{x}|}{2}\operatorname{Re}\int_{-1}^{1}\log\big(\mathcal{Z}(\xi) - \boldsymbol{\varkappa c}_m\big)\,\mathrm{d}\xi,$$

the latter of which we may employ quadrature on.

Assembly and solution

Recalling now our assumed property of independence of modes in the potential, that we may write it as the superposition $\Phi(t;\boldsymbol{x}) = \boldsymbol{U}(t)\cdot\boldsymbol{\phi}(\boldsymbol{x})$, we impose the boundary condition of impermeability—no fluid shall cross the boundary $\partial\Omega$. In other words, the fluid displaced by the movement of the body, must at the boundary itself move with that velocity, so that

$$\hat{\boldsymbol{n}}\cdot\nabla\Phi = \boldsymbol{U}\cdot\hat{\boldsymbol{n}}, \qquad \text{on } \partial\Omega.$$

By the product rule, and by virtue of $\boldsymbol{U}$ not being a function of the spatial variable, we have through the commutativity of the inner product that $\boldsymbol{U}\cdot\big(\hat{\boldsymbol{n}}\cdot\nabla\boldsymbol{\phi}(\boldsymbol{x})\big) = \boldsymbol{U}\cdot\hat{\boldsymbol{n}}$. In other words, we have the boundary condition that for each mode j of the potential,

$$\hat{\boldsymbol{n}}\cdot\nabla\phi_j \equiv \partial_{\hat{\boldsymbol{n}}}\phi_j = \hat{n}_j, \qquad \text{on } \partial\Omega,$$

whence the normal vector in (4). As is clear from equation (5), we may approximate get the normal vector on a straight line segment from implementing $\hat{\boldsymbol{n}}^n = (\delta z_n - i\delta x_n)|\delta\boldsymbol{x}|^{-1}$, where $\delta\boldsymbol{x} = \delta x_n + i\delta z_n$, as is done in the `normal_vector` method in the `IntegralEquation` class. The sixth normal vector, coinciding with rotation about the y-axis, is given by $\hat{n}_6{}^n = \boldsymbol{\varkappa c}_n \times \hat{\boldsymbol{n}}^n$, where the multiplication sign here indicates the cross product. The method `assemble_h` constructs the matrix representing the integral of the logarithm with a call to the `quad` method in the `Quadrature` class. The actual right-hand side of the integral equation is then calculated with a call to the method `right_hs`, choosing a mode, returning `right_hs` = `assemble_h@n_i`. Importing `linalg` from `numpy`, we may solve $\boldsymbol{\varphi}_j = \mathtt{\Theta}^{-1}\mathtt{h}$ for each of the modes. This is implemented in the `solve` method, constructing `Θ` and `h` only once, then calling `right_hs` three times, to return the tuple $[\boldsymbol{\varphi}_1, \boldsymbol{\varphi}_2, \boldsymbol{\varphi}_3]$.

Approximated added mass

Now having an approximation of $\boldsymbol{\phi}$, we may now approximate the integral in equation (2) as follows.

$$\mathfrak{m} = [m_{ij}] \approx \varrho\sum_{n=1}^{N}\phi_j{}^n\hat{n}_i{}^n\delta S_n$$

We are only interested in the substantive added mass, so we implement unit density. The added mass is then implemented as the `added_mass` method in the `IntegralEquation` class.

Added mass of a circle

Let a be the radius of the circle. We then have that its potential as a result of horizontal translation is given by

$$w = a^2U\mathcal{Z}^{-1} = \Phi + i\Psi, \quad \mathcal{Z} = x + iz. \tag{6}$$

We see that

$$\phi_1 = \operatorname{Re}\big(a^2U\mathcal{Z}^{-1}\big) = \frac{a^2U\cos\theta}{r^2}; \tag{7}$$

$$\phi_2 = \operatorname{Re}\big(a^2Ui\mathcal{Z}^{-1}\big) = \frac{a^2U\sin\theta}{r^2}. \tag{8}$$

By calculating the gradient of ϕ and transforming into polar coordinates, we find that

$$q_r = \frac{a^2U\cos\theta}{r^2}, \quad q_\theta = \frac{a^2U\sin\theta}{r^2}, \quad q^2 = \frac{a^4U^2}{r^4}.$$

We may now calculate the kinetic energy of the fluid by integrating over the entire fluid domain Ω,

$$T_{\text{fluid}} = \frac{\varrho}{2}\int_0^{2\pi}\int_a^\infty q^2 r\,\mathrm{d}r\mathrm{d}\theta = \frac{\pi\varrho a^2U^2}{2}.$$

Rotating the cylinder ought not induce drift in the fluid, as there is no mechanisms by which the fluid should be compelled to move from the circle turning. Because of the rotational symmetry of the circle, we must have that

$$\mathfrak{m} = [m_{ij}] = \begin{bmatrix}\pi\varrho a^2 & 0 & 0\\ 0 & \pi\varrho a^2 & 0\\ 0 & 0 & 0\end{bmatrix}.$$

We discretize the circle by defining

$$\mathtt{\Theta} = \mathtt{linspace}(0, 2\pi, \mathtt{N}+1), \quad \boldsymbol{x} = a\cos\mathtt{\Theta} + ia\sin\mathtt{\Theta}.$$

Implementing the potentials described in equation (7) and (8) in the `Potentials` class of `potentials.py`, we compare the numerical solution to the analytical potentials. In figures 3 and 4, we have used a fourth order quadrature scheme, and we see that there is seemingly negligible difference in the numerical solution and the theory.

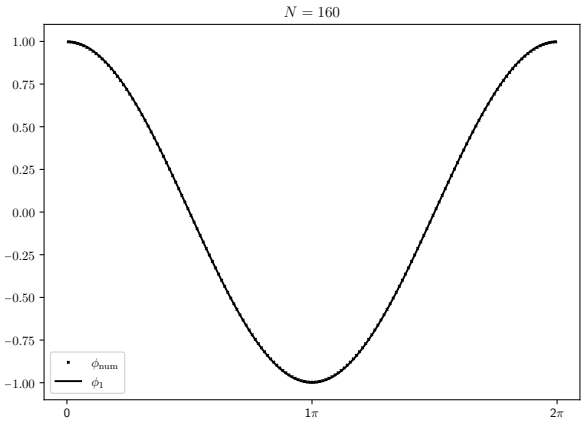

Figure 3: First mode of the potential for a circle using a fourth order quadrature scheme.

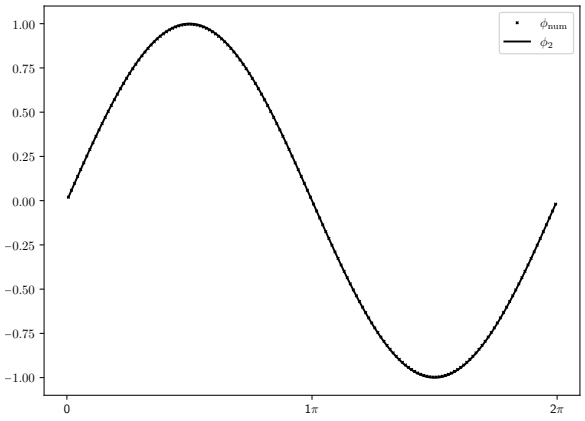

Figure 4: Second mode of the potential for a circle using a fourth order quadrature scheme.

The difference in accuracy for 2^{nd} and 4^{th} order quadrature schemes seems to be negligible. The L^2 error in the potentials is tabulated below in table 1, showing that the difference is at most in the thousandths.

[1] [4] Kennard, p.173

	2^{nd}		4^{th}	
N	ϕ_1	ϕ_2	ϕ_1	ϕ_2
32	0.1777	0.1727	0.1743	0.1690
64	0.0897	0.0884	0.0876	0.0862
96	0.0599	0.0594	0.0584	0.0579
128	0.0450	0.0447	0.0439	0.0435
160	0.0360	0.0358	0.0351	0.0349

Table 1: L^2 error differences in potential functions of a circle between second and fourther order Gauss–Lagrange quadrature.

We measure the error in the added mass absolutely, so that we just measure the absolute difference in the added mass. Since we set the the radius of the circle to be 1, a maximal difference of less than 0.05, as is indicated in figure 5, is fine, considering the added mass would simply be π.

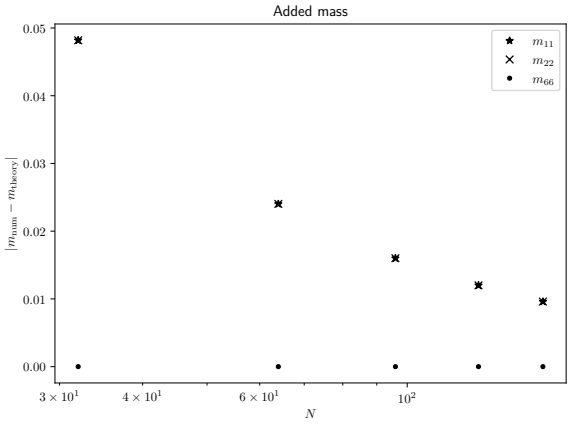

Figure 5: Absolute difference between the theoretical added mass m_{theory} and the calculated added mass m_{num}

We see that the convergence is pretty rapid, and that the code is performant.

Added mass of an ellipse

As with the circle, we will derive the analytical values for the added mass of an ellipse in motion. This derivation, unlike the circle, is not straight forward. And although we will employ the potential of the circle, elliptic coordinates will be introduced to transform this potential so that the ellipse can be studied. Also unlike the circle, because of its shape, the ellipse will actually have added mass in the sixth mode.

Elliptic coordinates

To study ellipses in the complex plane, we consider the ŽUKOVSKY transform[1]

$$\mathcal{z} = \mathcal{z}' + \frac{c^2}{\mathcal{z}'}, \qquad \mathcal{z}' = x' + iz', \tag{9}$$

so that $x' = r\cos\theta$, $z' = r\sin\theta$. Here the prime is no more than a decorator to differentiate the preimage of the ŽUKOVSKY transform from the complex numbers we will use. We now have for the complex variable $\mathcal{z} = x + iz$, whereupon using EULER's formula,[2]

$$x = \left(r + \frac{c^2}{r}\right)\cos\theta, \qquad z = \left(r - \frac{c^2}{r}\right)\sin\theta.$$

This is indeed an ellipse, as upon squaring both terms and adding them, we get that

$$\frac{x^2}{a^2} + \frac{z^2}{b^2} = 1, \quad a = r + \frac{c^2}{r}, \quad b = \left|r - \frac{c^2}{r}\right|.$$

We call a and b the major and minor semiaxes, corresponding to the longest and shortest semidiameters of the ellipse, respectively. The parameter $c = \sqrt{a^2 - b^2}$ is called the focus. Introducing now the elliptic complex variable ζ, defined by

$$\mathcal{z}' = ce^{\zeta}, \qquad \zeta = \xi + i\eta,$$

where $\xi = \ln(r/c)$ and $\eta = \theta$, we may express the complex number $\mathcal{z}$ in terms of this elliptic complex variable such that

$$\mathcal{z} = c\cosh\zeta = c\big(\cosh\xi\cos\eta + i\sinh\xi\sin\eta\big). \tag{10}$$

We now clearly see that cricles in $\mathcal{z}'$ are ellipses in $\mathcal{z}$. Lines of constant ξ constitute confocal ellipses, parametrized with η, whilst lines of constant η are confocal hyperbolas in ξ. We may eliminate either ξ or η in equation (10) to find that the major and minor semiaxes are respectively given by

$$a' = c\cosh\xi, \qquad b' = c|\sinh\xi|. \tag{11}$$

Combining now equations (10) and (11), we find that we may write

$$\xi = \ln\left(\frac{a' + b'}{c}\right), \qquad \xi \geq 0. \tag{12}$$

We will use this convention, that ξ be strictly nonnegative, though more discussion on this is to be found in KENNARD's work.[3] It is then apparent that the potential for a circle, described in equation (6), may be transformed to give

$$w = U\sqrt{\frac{a+b}{a-b}}(b\cos\alpha + ia\sin\alpha)e^{-\zeta}, \tag{13}$$

where α is the inclination of the ellipse relative to the direction of motion. That is, an angle $\alpha = 0$ corresponds to motion along x, and $\alpha = \pi/2$ corresponds to motion along z. Clearly, by virtue of the above discussion, the real part of the potential is given by

$$\Phi(\zeta;\alpha) = U\sqrt{\frac{a+b}{a-b}}(b\cos\alpha\cos\eta + a\sin\alpha\sin\eta)e^{-\xi},$$

so that $\phi_1(\zeta) = \Phi(\zeta;0)$ and $\phi_2(\zeta) = \Phi(\zeta;\pi/2)$.

Translatory kinetic energy

The scale factor of the elliptic coordinate system can be shown to be equal to

$$h_\xi = c\sqrt{\sinh^2\xi + \sin^2\eta} = \sqrt{b'^2 + c^2\sin^2\eta}.$$

Since $q_\xi = -{h_\xi}^{-1}\partial_\xi\Phi = {h_\xi}^{-1}\Phi$, and that change in ξ corresponds to a change in $\hat{\boldsymbol{n}}$, we must have that $q_\xi = q_{\hat{\boldsymbol{n}}}$, where $q_{\hat{\boldsymbol{n}}} = -{h_\xi}^{-1}\partial_{\hat{\boldsymbol{n}}}\Phi$. In turn, we have that

$$q_\xi = U\left(\frac{a+b}{a'+b'}\right)\frac{b\cos\alpha\cos\eta + a\sin\alpha\sin\eta}{h_\xi}.$$

Considering the kinetic energy of the fluid, using GAUSS' divergence theorem, and using the product rule, we find that

$$T_{\text{fluid}} = \frac{\varrho}{2}\int_\Omega q^2\,\mathrm{d}V = -\frac{\varrho}{2}\int_{\partial\Omega}\Phi q_{\hat{\boldsymbol{n}}}\,\mathrm{d}S. \tag{14}$$

Letting ξ_0 denote the value of which ξ lies on the ellipse, we assert that such points be represented by $\mathcal{z}_0 = a\cos\eta + ib\sin\eta$. We then have from equation (12) that $a' = a$ and $b' = b$ on the ellipse, and that

$$\exp(\xi_0) = \frac{a+b}{c} = \frac{a+b}{a-b}, \quad \exp(-\xi_0) = \frac{a-b}{a+b}.$$

From the relation that $q_{\hat{\boldsymbol{n}}} = \partial_s\Psi$,[4] and that $\mathrm{d}\Psi = -\partial_\xi\Phi\mathrm{d}\eta$,

$$T_{\text{fluid}} = \frac{\varrho U^2}{2}\int_0^{2\pi}(b\cos\alpha\cos\eta + a\sin\alpha\sin\eta)^2\,\mathrm{d}\eta$$

Calculating the integral, we find that the kinetic energy is given by

$$T_{\text{fluid}} = \frac{\varrho\pi U^2}{2}(b^2\cos^2\alpha + a^2\sin^2\alpha).$$

When $a = b$, the ellipse is a circle, and we observe the kintetic energy is what we got for the circle.

[2] [4] KENNARD, pp.190–192
[3] [4] KENNARD sect.82, pp.192–196
[4] [5] LAVRENTEV & ŠABAT, p.233

Rotational kinetic energy

Consider the complex variable defined as in equation (10), with a potential

$$w = iAe^{-2\zeta}, \qquad \Psi = Ae^{-2\zeta}\cos 2\eta,$$

where A is some parameter to be determined. The stream function satisfies the condition that[1]

$$\Psi - \frac{\omega\big(x^2+z^2\big)}{2} = C,$$

where C is some constant. We recall that $\mathfrak{z} = x+iz$, so that

$$Ae^{-2\zeta}\cos 2\eta - \frac{c^2\omega\big(\cosh 2\xi + \cos 2\eta\big)}{4} = C.$$

We evaluate this at the ellipse ξ_0, so that we eliminate A and ξ, yielding

$$w = \frac{i\omega(a+b)^2}{4e^{2\zeta}}, \quad \Phi = \frac{\omega c^2 \sin 2\eta}{4}.$$

We may then again use the formulation of the kinetic energy of the fluid as it was presented in equation (14), noting that the differential element $\mathrm{d}\Psi$ brings with a factor 2, yielding

$$T_{\text{fluid}} = \frac{\varrho\omega c^4}{16}\int_0^{2\pi}\sin^2 2\eta\,\mathrm{d}\eta = \frac{\pi\varrho\omega c^4}{16}.$$

Added mass

The added mass can them be found.

$$\mathbf{m} = \begin{bmatrix} \pi\varrho b^2 & 0 & 0 \\ 0 & \pi\varrho a^2 & 0 \\ 0 & 0 & \pi/8\varrho c^4 \end{bmatrix}$$

Elliptic integrals

To carry on with the analysis, we will need to introduce the elliptic integrals. Although it will seem unmotivated to introduce them without much explanation as to what they represent, their applications will become clear in the following sections. With that said, we introduce the incomplete elliptic integral of the first kind,[2]

$$\mathrm{F}(\varphi|k) = \int_0^{\varphi}\frac{1}{\sqrt{1-k^2\sin^2\theta}}\,\mathrm{d}\theta \tag{15}$$

The *incomplete* denomination refers to the amplitude φ. By setting $\varphi = \pi/2$, we have complete elliptic integral of the first kind,

$$\mathrm{K}(k) = \mathrm{F}(\pi/2|k) = \int_0^{\pi/2}\frac{1}{\sqrt{1-k^2\sin^2\theta}}\,\mathrm{d}\theta \tag{16}$$

We also have the incomplete elliptic integral of the second kind,

$$\mathrm{E}(\varphi|k) = \int_0^{\varphi}\sqrt{1-k^2\sin^2\theta}\,\mathrm{d}\theta, \tag{17}$$

and the complete variant, which we will simply label $\mathrm{E}(k) \equiv \mathrm{E}(\pi/2|k)$. We call $\kappa = k^2$ the parameter, and introduce the complementary parameter $\kappa' = 1-\kappa$—with it the notation that $\mathrm{K}'(k) = \mathrm{K}(k')$, and $\mathrm{E}'(k) = \mathrm{E}(k')$—$k$ is named the parameter and $k' = \sqrt{\kappa'}$ is its complement.

Jacobi introduced the following set of equations, upon writing $x = \mathrm{F}(\varphi|k)$ and $\varphi = \mathrm{am}(x)$.

$$\mathrm{sn}\,x = \sin\varphi, \qquad \mathrm{cn}\,x = \cos\varphi; \tag{18}$$

$$\mathrm{dn}\,x = \sqrt{1-k\sin^2\varphi} \tag{19}$$

This set, and variations thereof, is simply referred to as Jacobi elliptic functions, and their individual names are *sinus amplitudinis*, *cosinus amplitudinis*, and *delta amplitudinis*, respectively. These functions will be explained further in later sections.

The arithmetic-geometric mean

The arithmetic-geometric mean provides a swift way to calculate elliptic integrals numerically. Its formulation seems rather arbitrary, but we will quickly see that there is a foundational connection between them. Further reading is highly encouraged, in particular *Pi and the AGM*[3] by the Borwein brothers. Following the literature, we define the arithmetic geometric mean M of a and b through the iterative process

$$a_n = \frac{a_{n-1}+b_{n-1}}{2}, \qquad b_n = \sqrt{a_{n-1}b_{n-1}}.$$

This process is maintained until $c_n = 1/2(a_{n-1} - b_{n-1}) < \varepsilon$, where ε is the desired accuracy. We have assumed that $0 < b_0 \leq a_0$, and we may observe that it is always true that $b_{n-1} \leq b_n \leq a_n \leq a_{n-1}$, so that the values have a common limit. This limit is the arithmetic-geometric mean:

$$M(a,b) = \lim_{n\to\infty} a_n = \lim_{n\to\infty} b_n.$$

It is evident that from this definition, the starting the algorithm at some later iteration must result in the same function. In other words,

$$M(a,b) = M\left(\frac{a+b}{2}, \sqrt{ab}\right).$$

The arithmetic-geometric mean is also obviously homogeneous, meaning $M(\lambda a, \lambda b) = \lambda M(a,b)$, where $\lambda > 0$. It may be shown that[4]

$$\frac{\pi}{2M(1,\mathfrak{z})} = \int_0^{\pi/2}\frac{1}{\sqrt{1-\big(1-\mathfrak{z}^2\big)\sin^2\theta}}\,\mathrm{d}\theta.$$

[1] [4] Kennard, p.246
[2] [1] Abramowitz & Stegun, eq.17.2.6, p.589
[3] [2] Borwein & Borwein
[4] [2] Borwein & Borwein, pp.5–7

A full proof is not appropriately reproduced in this text, so the reader is referred to the Borwein brothers' book. The relation to elliptic integrals is now quite apparent, in particular

$$\mathrm{K}(k) = \frac{\pi}{2M(1,k')}, \quad \frac{\mathrm{E}(k)}{\mathrm{K}(k)} = 1 - \sum_n 2^{n-1} {c_n}^2.$$

These are the `K` and `E` methods implemented in the `Jacobi` class of `jacobi.py`. Ever yet, we intriduce two auxiliary functions

$$I(a,b) = \int_0^{\pi/2} \frac{1}{\sqrt{a^2\cos^2\theta + b^2\sin^2\theta}}\,\mathrm{d}\theta; \qquad (20)$$

$$J(a,b) = \int_0^{\pi/2} \sqrt{a^2\cos^2\theta + b^2\sin^2\theta}\,\mathrm{d}\theta. \qquad (21)$$

We note that $I(a,b) = {}^1\!/_a\,\mathrm{K}'\left({}^b\!/_a\right)$, and $J(a,b) = a\,\mathrm{E}'\left({}^b\!/_a\right)$. It may be shown that these functions satisfy

$$I(a_{n+1}, b_{n+1}) = I(a_n, b_n);$$
$$2J(a_{n+1}, b_{n+1}) - J(a_n, b_n) = a_n b_n I(a_n, b_n).$$

Discretizing the ellipse

There are multiple ways to approach discretizing the ellipse, the most apparent of which being

$$\boldsymbol{x} = a\cos\eta + ib\sin\eta, \qquad \eta \in [0, 2\pi), \qquad (22)$$

where the parameter η is the very same as the elliptic coordinate, called the *eccentric* variable. It is indeed related to the polar variable, as is clear upon considering $\tan\eta$. This value is equal to ${}^{az}\!/_{bx}$, by the geometric interpretation of the tangent, where $\boldsymbol{x} = x + iz$. For a polar representation

$$\boldsymbol{x} = r\cos\theta + ir\sin\theta, \qquad \theta \in [0, 2\pi), \qquad (23)$$

we find that

$$\tan\eta = {}^a\!/_b\tan\theta, \quad r(\theta) = \frac{ab}{\sqrt{b^2\cos^2\theta + a^2\sin^2\theta}}.$$

For the circle, when $a = b$, the eccentric and polar angles are of course equal. We plot the relationship between the eccentric and polar variables, illustrated in figure 6.

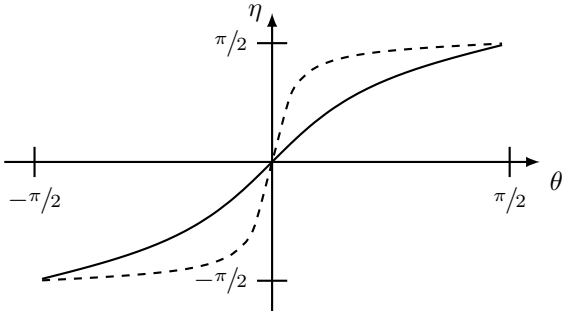

Figure 6: Relationship between the eccentric variable η and polar variable θ. Dashed line is $b = {}^a\!/_{10}$, whole line is $b = {}^a\!/_2$.

We may discretize θ into a `linspace`, an array of equally spaced points of the interval $[0, 2\pi)$, and plot the coordinates of the ellipse according to equation (23), as is done in figure 7 below.

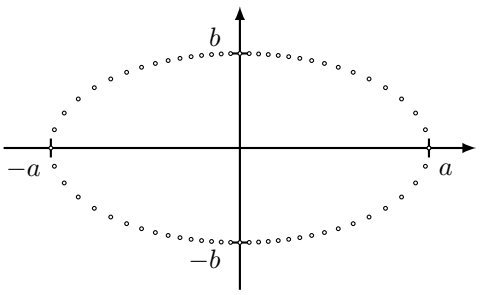

Figure 7: Ellipse parametrized with the polar variable θ, according to equation (23).

We see that the points tend to accumulate at the top of the ellipse, which indeed makes sense. As we change the polar angle by an equal amount counter-clockwise, the arc length drawn out between points will diminish towards ${}^\pi\!/_2$. This is illustrated in figure 8 below, where points on the ellipse for integer multiples of ${}^\pi\!/_8$ are plotted in the first quadrant.

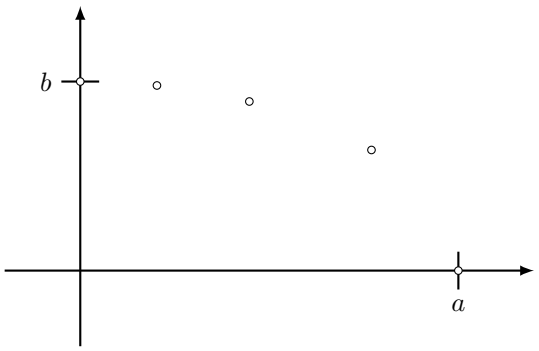

Figure 8: Demonstration that the arc length between points decreases counter-clockwise in the first quadrant as the polar angle θ approaches ${}^\pi\!/_2$.

This is not the case for the ellipse discretized according to equation (22), using the eccentric variable η, as is seen in figure 9 below.

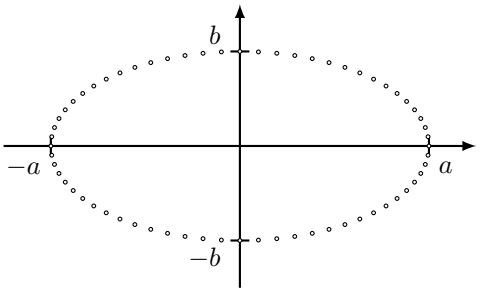

Figure 9: Ellipse parametrized with the eccentric variable η, according to equation (22).

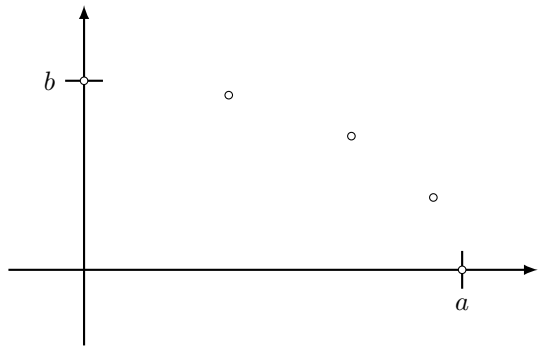

Figure 10: Arc length increases counter-clockwise in the first quadrant as the eccentric variable η approaches $\pi/2$.

Of interest to investigate is how these distributions of nodes impact the convergence of the software—one thought is that performance of tendency for nodes to concentrate towards either of the semiaxes will positively impact the accuracy for the corresponding mode. To be investigated is also whether a distribution such that arc lengths between nodes remain constant over the whole ellipse will perform better than either the eccentric or polar representation.

We wish to find a set of N points on the ellipse such that the arc length between successive points is constant. The arc length of a curve parametrized by $\boldsymbol{y}(x)$ is given by

$$\ell(a;b) = \int_a^b |\boldsymbol{y}'(x)|\,\mathrm{d}x, \qquad 0 \leq a \leq b,$$

where a and b are the start and end points of the parametrization, and their ordering is convention for the sake of clarity. Note that we may write $\ell(a;b) = \ell(0;b) - \ell(0;a) \equiv \ell(b) - \ell(a)$. Finding then the arc length from $\eta = 0$ to some value, say t, using equation (22), yields the integrand $\sqrt{a^2\cos^2\eta + b^2\sin^2\eta}$. We may use the Pythagorean identity that $\cos^2\eta + \sin^2\eta = 1$, which yields

$$\ell(\eta) = a\int_0^\eta \sqrt{1 - k^2\sin^2\eta}\,\mathrm{d}\eta, \qquad k^2 = 1 - \frac{b^2}{a^2},$$

which is exactly the incomplete elliptic integral of the second kind, as written in equation (17). We now consider the perimeter of the ellipse. Due to the symmetry of the ellipse—or the periodicity of the elliptic functions—it is evident that the perimeter is given by $\ell(2\pi) = 4\,\mathrm{E}(k)$. We may then find the set of angles such that N nodes of equal arc lengths are placed on the ellipse by the relation that

$$\mathrm{E}(\eta_n|k) = \frac{4n\,\mathrm{E}(k)}{aN}, \qquad n \in \{1,\ldots,N\}.$$

By an arithmetic-geometric mean algorithm, we may find the angles η.

Added mass of a square

Å skulle diskretisere kvadratet er ikke like trivielt som sirkelen eller ellipsen. Vi ønsker å skulle kunne gjenbruke samme klasse for integrallikningen, så en polar implementering av diskretiseringen er mest opplagt. En kontinuerlig mulighet er en såkalt superellipse, som kan diskretiseres med

$$\boldsymbol{x}(\theta) = \left(|\cos\theta|^{2/N}\,\mathrm{sgn}\,(\cos\theta), |\sin\theta|^{2/N}\,\mathrm{sgn}\,(\sin\theta)\right),$$

som vil konvergere raskt mot et kvadrat når N blir stor. Problemet her er at θ ikke faktisk er vinkelen i parametriseringen. Parametriseringsvariablen vil bruke lang tid i hjørnene på superellipsen, og en enorm andel av normalvektorene langs randa vil derfor være fullstendig feil.

En enklere løsning vil være å heller kjøre θ gjennom `if`-sjekker, som følger.

Algorithm 2 Konstruer kvadrat

for $n \leq$ `N` **do**
  if $\theta_n \in [-\pi/4, \pi/4)$ **then**
    $\boldsymbol{x}_n, \boldsymbol{y}_n \leftarrow 2a, 2a\tan(\theta_n)$
  else if $\theta_n \in [\pi/4, 3\pi/4)$ **then**
    $\boldsymbol{x}_n, \boldsymbol{y}_n \leftarrow 2a\sec(\theta), 2a$
  else if $\theta_n \in [3\pi/4, 5\pi/4)$ **then**
    $\boldsymbol{x}_n, \boldsymbol{y}_n \leftarrow -2a, -2a\tan(\theta_n)$
  else if $\theta_n \in [5\pi/4, 7\pi/4)$ **then**
    $\boldsymbol{x}_n, \boldsymbol{y}_n \leftarrow -2a\sec(\theta), -2a$
  end if
end for

Denne løsningen er ikke veldig vakker, men den forsikrer at alle nodene faktisk ligger på kvadratet. Dette kan ikke sies for hjørnene i $\boldsymbol{\varkappa}$, ettersom hjørnenodene kan havne innenfor randa i dersom ikke enten $\boldsymbol{x}_p$ eller $\boldsymbol{x}_m$ ligger akkurat i hjørnet for denne N-verdien. Vi ser i figur 11 at dette kan føre til merkelige mønstre i konvergensen til den adderte massen, hvor tilnærmingen faktisk kan bli dårligere for en større N-verdi.

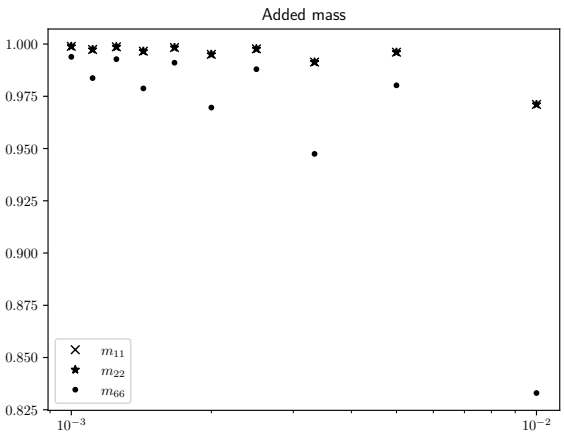

Figure 11: Numerisk utregnet over teoretisk addert masse på et kvadrat.

Samtidig ser vi at den utregnede adderte massen fakitsk konvergerer. Vil man unngå å se denne unøyaktigheten, kan man forsikre seg at $\{\pi/4, 3\pi/4, 5\pi/4, 7\pi/4\} \in \theta$ ved å la N alltid være delelig på 8, slik som i figur 12.

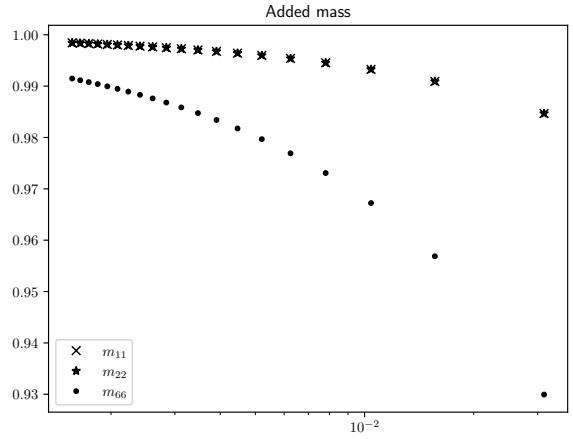

Figure 12: Numerisk utregnet over teoretisk addert masse på et kvadrat med N delelig på 8.

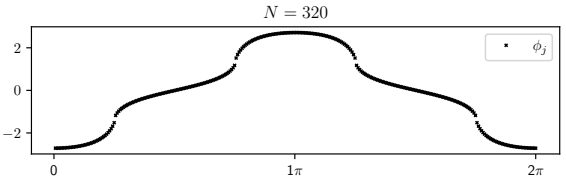

Figure 13: ϕ_1 er gitt numerisk med punkter.

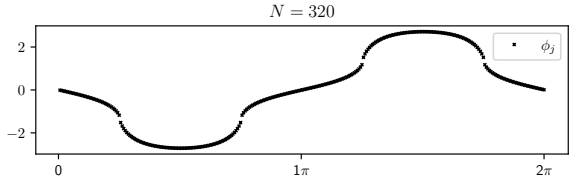

Figure 14: ϕ_2 er gitt numerisk med punkter.

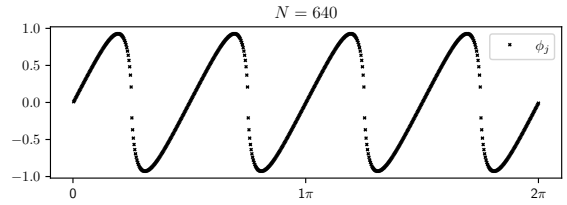

Figure 15: ϕ_6 er gitt numerisk med punkter.

References

[1] Abramowitz, Milton and Stegun, Irene A. *Handbook of Mathematical Functions*. 3rd ed. National Bureau of Standards, 1965.

[2] Borwein, Jonathan Michael and Borwein, Peter Benjamin. *Pi and the AGM*. Wiley-Interscience, 1987.

[3] Darwin, Charles Galton. "Note on Hydrodynamics". In: *Proceedings of the Cambridge Philosophical Society* 49 (1953), pp. 342–354.

[4] Kennard, Earle H. *Irrotational Flow of Frictionless Fluids, Mostly of Invariable Density*. U.S. Government Printing Office, 1967.

[5] Lavrentev, Mihail Alekseyevič (Лаврентьев) and Šabat, Boris Vladimirovič (Шабат). *Methoden der komplexen Funktionentheorie*. VEB Deutscher Verlag der Wissenschaften, 1967.

[6] Markuševič, Aleksey Ivanovič (Маркушевич). *Theory of Functions of a Complex Variable, Volume II*. Ed. by Richard A. Silverman. Prentice-Hall, inc., 1965.

[7] Milne–Thomson, Louis Melville. *Theoretical Hydrodynamics*. Macmillan & co. ltd., 1968.